Moment canting in 3d-based amorphous ferromagnets

1993 J. Phys.: Condens. Matter 5 3275

(http://iopscience.iop.org/0953-8984/5/19/023)

J. Phys.: Condens. Matter 5 (1993) 3275–3288. Printed in the UK

Moment canting in 3d-based amorphous ferromagnets

Q A Pankhurst† and M R J Gibbs‡

† Department of Physics, University of Liverpool, Liverpool L69 3BX, UK
‡ School of Physics, University of Bath, Bath BA2 7AY, UK

Received 22 December 1992, in final form 2 March 1993

Abstract. The available evidence both for and against the existence of non-collinear spin structures in 3d-based amorphous ferromagnets is assessed, and supplemented with the results of an extended ^{57}Fe Mössbauer study of two series of post-production treated materials. Mössbauer spectra of as-received, stress-relieved and field-annealed ribbons of $Fe_{78}B_{13}Si_9$ and $Fe_{40}Ni_{40}B_{20}$ were recorded in zero applied field at room temperature for a number of angles of inclination between the γ-ray beam and the normal to the ribbon plane. The resultant data were compared with four different moment distribution models: (i) a single uniform moment, (ii) an ellipsoidal distribution, (iii) a wedge-shaped distribution, and (iv) a two-moment domain model. None of these models provided an adequate description of the non-annealed ribbons, whereas model (iii) fitted the annealed $Fe_{78}B_{13}Si_9$ ribbons and model (iv) fitted the annealed $Fe_{40}Ni_{40}B_{20}$ ribbons. It is concluded that there is cumulative evidence in favour of ambient non-collinear spin structures in some annealed as well as non-annealed metallic glasses, but that the scale of the moment correlation lengths remains unresolved.

1. Introduction

The spin structures in 3d-based amorphous ferromagnets are being examined using a number of techniques. From recent published results it appears that the spins are not collinear over the length scales typical of conventional 3d-based crystalline ferromagnets. It is argued that the length scales are much shorter, and there are indications that the correlation length may be as short as the interatomic spacing. While further detailed experiments continue, it is important to assess the evidence, and to establish consistent trends. This is particularly true in the case of sample history. In this paper we draw together the available evidence, supplementing this with some of our own Mössbauer effect measurements, in order to bring some qualitative understanding to this problem. The studies are not only of academic interest, requiring new models for the magnetic structures which can be supported on a non-crystalline lattice, but also of technical significance. The use of 3d-based amorphous materials in transducers where the magnetostrictive or magnetoelastic response is invoked, will be degraded if the moments are not collinear. An understanding of the factors controlling the canting, and routes to minimize the effect must be established.

The available data from four main categories of measurement are summarized in table 1 [1–9]. The polarized neutron and Mössbauer experiments can be categorized as direct measurements, whereas the remainder are indirect. This division is in terms of what the measurements probe within the sample. In direct measurements, a volume of material is irradiated, and a signal is detected with components from all sources within that volume. For magnetostriction measurements, the signal comes only from those parts of the sample influenced by the fields applied (typically a few thousand A m^{-1}), and in domain studies

Table 1. Previously published data for moment canting in Fe-based amorphous ferromagnets, measured via polarized neutron scattering, Mössbauer spectroscopy, magnetostriction and domain imaging. Post-production treatment, namely stress relief (SR) or field anneal (FA), is indicated. The polarized neutron data was obtained at 10 K in a field of $B = 2$ T. With a few exceptions, the Mössbauer results were recorded at room temperature in zero field. Magnetostriction measurements were made at room temperature in fields of a few kA m^{-1}. Domain images were recorded at room temperature in zero field and in fields of 400 A m^{-1} (5 Oe in cgs).

Composition and post-production treatment		Polarized neutrons[a]	Mössbauer[b]		Magneto-striction[c]	Domain imaging[d]
			In-plane	Out-of-plane		
$Fe_{86}B_{14}$	As cast			$\leqslant 22°$[e] [3]		
$Fe_{83}B_{17}$	As cast	30° ± 6° [1]				
$Fe_{80}B_{20}$	As cast			$\leqslant 18°$[e] [3]		
$Fe_{78}B_{12}Si_{10}$	As cast	14° ± 15° [1]				
$Fe_{78}B_{13}Si_9$	As cast	0° ± 7° [1]	±118°	±43° [4]	±90° [7]	
			±71°	±32° [5]		
	SR	0° ± 7° [1]	±57°	±21° [5]		
	FA		±50°	±20° [6]	±10° [7]	
			±30°	±20°[f] [6]	±10° [8]	
$Fe_{76}B_{12}Si_{12}$	As cast	21° ± 5° [1]				
$Fe_{75}B_{15}Si_{10}$	As cast	16° ± 11° [1]				
$Fe_{67}Co_8B_{14}Si$						±15° [9]
$(Fe_{0.75}Ni_{0.25})_{78}B_{12}Si_{10}$	As cast	26° ± 6° [2]				
$Fe_{40}Ni_{40}B_{20}$	FA				0° [8]	
$(Fe_{0.5}Ni_{0.5})_{78}B_{12}Si_{10}$	As cast	32° ± 4° [2]				
$(Fe_{0.25}Ni_{0.75})_{78}B_{12}Si_{10}$	As cast	34° ± 4° [2]				
$(Fe_{0.125}Ni_{0.875})_{78}B_{12}Si_{10}$	As cast	30° ± 4° [2]				
$Fe_5Co_{75}B_{15}Si_5$	As cast		±113°	±29° [4]		

[a] Root mean square canting angle derived from the measured mean square moment, $\langle \mu_x^2 \rangle$, transverse to the applied field.

[b] Analysed according to a wedge-shaped moment distribution model [6] with in-plane and out-of-plane angular limits for the distribution.

[c] Standard deviation of an assumed Gaussian distribution of moment directions about the measuring field direction.

[d] Limit of the angular deviation of the observed sub-domains about the mean magnetization direction.

[e] At 4.2 K in applied fields of 2 T $\leqslant B \leqslant$ 6 T. Harker and Pollard [3] measured the mean square of the sine of the angle between the moments and the applied field, $\langle \sin^2 \alpha \rangle$. The limiting angle tabulated is obtained if one assumes a uniform distribution of the moments over a cone centred on the applied field direction.

[f] In an applied field of $H = 280$ A m^{-1} (3.5 Oe in cgs units).

there is spatial averaging from the colloid (typically to length scales of tens of microns). The distinction is important in providing an explanation of the results.

It is also important to distinguish between those experiments that have been performed in external fields of sufficient strength to remove all domains, and those performed under *ambient conditions of zero applied field and room temperature.* All of the polarized neutron data [1, 2] have been collected at 10 K in a field of 2 T. In all cases, except the $Fe_{78}B_{13}Si_9$, there is evidence of substantial moment canting in the as-received state. Mössbauer measurements on $Fe_{86}B_{14}$ and $Fe_{80}B_{20}$ at 4.2 K in applied fields up to 6 T are consistent with up to half the degree of canting observed in the polarized neutron experiments [3]. In contrast, the room temperature DC hysteresis loop of any of the alloys listed, even in the as-received state where there are substantial variations in local anisotropy due to casting stresses, show > 99% saturation in fields of the order of 0.03 T. However, studies of the law of approach to magnetic saturation, in fields up to 4 T, show that the susceptibility is

higher than expected for paraprocesses [10]. Recent room temperature studies [11] up to 20 T on as-received $Fe_{80}B_{20}$ and $Fe_{78}B_{13}Si_9$ show that the susceptibility is higher than in polycrystalline nickel, indicating that moment rotation continues at very high fields. This cumulative evidence indicates that full magnetic saturation with all of the moments aligned with the field, within the effects of thermal fluctuation, cannot be achieved. In all laboratory scale fields there are moments capable of rotation.

There have also been a number of reported zero-applied-field measurements, particularly Mössbauer effect measurements [4–6]. Although such experiments do not provide immediate information on the question of moment canting in applied fields, they are nevertheless very useful, both for sample characterization, as well as for comparing the direct and indirect measurement techniques. This is particularly true for field-annealed samples, where the magnetostriction and domain imaging data show near perfect moment collinearity along a macroscopically induced in-plane easy axis direction. Zero-field Mössbauer measurements on field-annealed samples are consequently very similar in concept to applied-field polarized neutron measurements on as-received samples.

Inferences may also be drawn from the zero-field measurements on non-annealed ribbons. The Mössbauer data on $Fe_{78}B_{13}Si_9$ shows a magnitude of moment canting that is comparable with that observed for neutron studies on other compositions, although not with the neutron data on the same composition. Anomalies such as this may be attributable to the differences between batches of the same composition, in the sense that the overall aging profiles before measurement are unlikely to be the same. One might draw the general conclusion that, within these discussed limits, the Mössbauer and neutron studies are probing and demonstrating the same high degree of moment canting.

In order to resolve some of the outstanding anomalies discussed above, we report here zero-field data on a single batch of $Fe_{78}B_{13}Si_9$ and a single batch of $Fe_{40}Ni_{40}B_{20}$ which have been studied both with direct and indirect probes. We have chosen the Mössbauer technique as the direct study, and have already reported the details of the indirect magnetostriction studies [8]. Further applied field Mössbauer measurements are in progress and will be reported elsewhere in due course.

The principle of the Mössbauer technique as applied to the measurement of moment distribution functions is as follows. In a standard six-line ^{57}Fe Mössbauer spectrum, the relative areas of the outer:middle:inner pairs of lines are $3:r:1$, where r depends on the angle between the γ-ray beam and the individual magnetic moments. In a metallic glass there is a distribution of moment directions, and therefore a superposition of contributions to r. By analysing r as a function of the angle between the γ-ray beam and the ribbon plane, it is possible to determine the moment distribution function.

However, in practice the deconvolution problem is rather complicated. Firstly, careful fitting procedures are needed to extract r reliably. The effect of non-zero electric quadrupole interactions on the spectral lines should be incorporated [12], and possible thickness effects considered [13]. Secondly, an appropriate model for the moment distribution is needed. To date many models have been proposed and used to analyse what are, in general, rather limited suites of data. There is comparatively little published work in which a variety of distribution models are considered and their relative merits determined. Consequently, in this paper we have chosen to test four different moment distribution models against a set of data obtained from over sixty Mössbauer spectra of a range of post-production-treated metallic glass samples. Our objective is to arrive at some definitive conclusion about the nature of the moment distributions in the ribbons, and the efficacy of the Mössbauer effect when it is used in this way.

2. Experimental details

Commercially available alloys were used in this study: METGLAS 2605-S2 ($Fe_{78}B_{13}Si_9$) and VAC 0040 ($Fe_{40}Ni_{40}B_{20}$)†. Samples were cut from 25 mm wide, 25 μm thick source material. The METGLAS samples were cut to be 45 mm long by 25 mm wide, and the VAC samples were 45 mm long by 15 mm wide. Stress relief was carried out by heating in air: 40 min at 400 °C for the METGLAS ribbons, and 10 min at 350 °C for the VAC ribbons. Field annealing was accomplished with a field of 0.4 T directed along the length or across the width of the samples. The METGLAS samples were field annealed for 40 min at 400 °C, and the VAC samples were annealed for 10 min at 350 °C. These times and temperatures were chosen to be consistent with earlier work [8] in terms of optimizing stress relief and minimizing moment canting.

Conventional ^{57}Fe Mössbauer spectra were recorded at room temperature using an unpolarized ^{57}CoRh source. (In future experiments we intend to use a polarized ^{57}CoFe Mössbauer source.) For each sample, a series of spectra were recorded for a number of γ-ray propagation directions in the xz and yz planes, where the xyz coordinate system is defined with respect to the ribbon axes, with the x axis parallel to the long axis of the ribbon, and the z axis normal to the ribbon plane. This experimental geometry is illustrated in figure 1. A variable angle mount was used in which the ribbons were sandwiched between a lead mask and a perspex plate, in an attempt to provide a sample environment that was both controllable and stress-free. Care was taken to ensure that the samples were not exposed to any stray magnetic fields, both before and during the data collection. The measurements were therefore made at an effective field close to zero. Future work will involve the application of magnetizing fields.

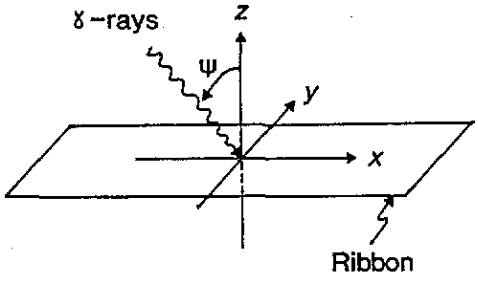

Figure 1. Experimental geometry for the transmission Mössbauer experiments, showing the xyz coordinate system, and the γ-ray beam direction, with respect to the metallic glass ribbon sample.

A typical set of Mössbauer spectra are shown in figure 2. The very high signal-to-noise ratios evident in the data were obtained by counting for not less than eight hours per spectrum with a high activity ($\sim$ 50 mCi) source. Spectra were recorded using a triangular velocity waveform, and were folded to obtain data without baseline curvature. Calibration is with respect to α-Fe at room temperature.

3. Results and analysis

The spectra were fitted using six Voigtian line profiles (Gaussian distributions of Lorentzian lines) whose positions were constrained to be physically realistic following the method of

† METGLAS is the registered trademark of Allied Corporation, and VAC is the registered trademark of Vacuumschmelze GmbH.

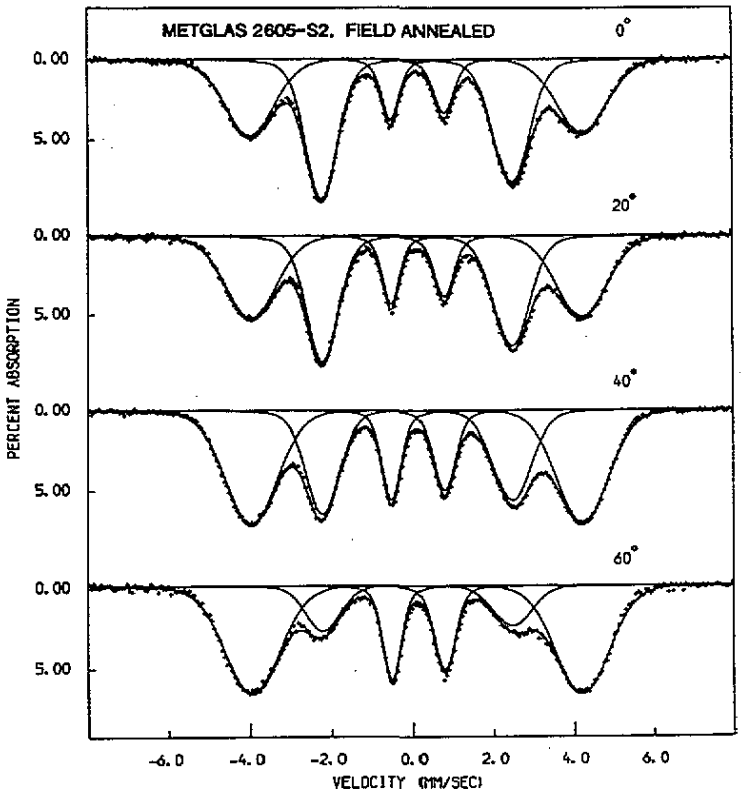

Figure 2. Room temperature Mössbauer spectra of a sample of $Fe_{78}B_{13}Si_9$ (METGLAS 2605-S2) that had been field-annealed in the x direction. The ribbon was inclined at an angle of $\psi_{xz} = 0°$, 20°, 40° and 60° to the γ-ray beam, in the xz plane. The solid lines are the results of least-squares fits using a constrained set of six Voigtian line profiles.

Lines and Eibschütz [14]. The ratio of the areas of the outer:inner pairs of lines in the sextet was constrained to be 3:1. This is an assumption which is valid so long as thickness effects are not significant. The high quality of the fits obtained with the 3:1 area constraint, even in the extreme case of a 60° angle of inclination between the γ-ray beam and the z axis, support the validity of this assumption. As a further test for thickness effects, a 'double-thickness' spectrum was recorded using two ribbons in tandem. Again, the 3:1 area criterion was achieved, implying that in even this extreme case thickness effects were not noticeable. That thickness effects should be insignificant, despite the relatively high 25 μm thickness of the foils, is understandable given the wide spread in line positions in the Mössbauer spectrum. This line broadening, which is due to the distribution in local environments for the ^{57}Fe atoms, results in a reduction in the effective absorber thickness at any given velocity.

The fitted relative areas, r, of the second and fifth lines of the spectra are plotted in figures 3 and 4 as a function of ψ_{xz} and ψ_{yz}. Uncertainties in the values of r arising from the fitting procedure are estimated to be less than 1%. Three features are immediately apparent on visual inspection: (i) in no case does r attain the limiting value of 4.0, (ii) in all cases the maximum value of r occurs for $\psi = 0°$, and (iii) in all cases the variation of r as a function of ψ is different for inclinations in the xz and yz planes. The significance of these features are as follows. The relative areas of the outer:middle:inner pairs of lines

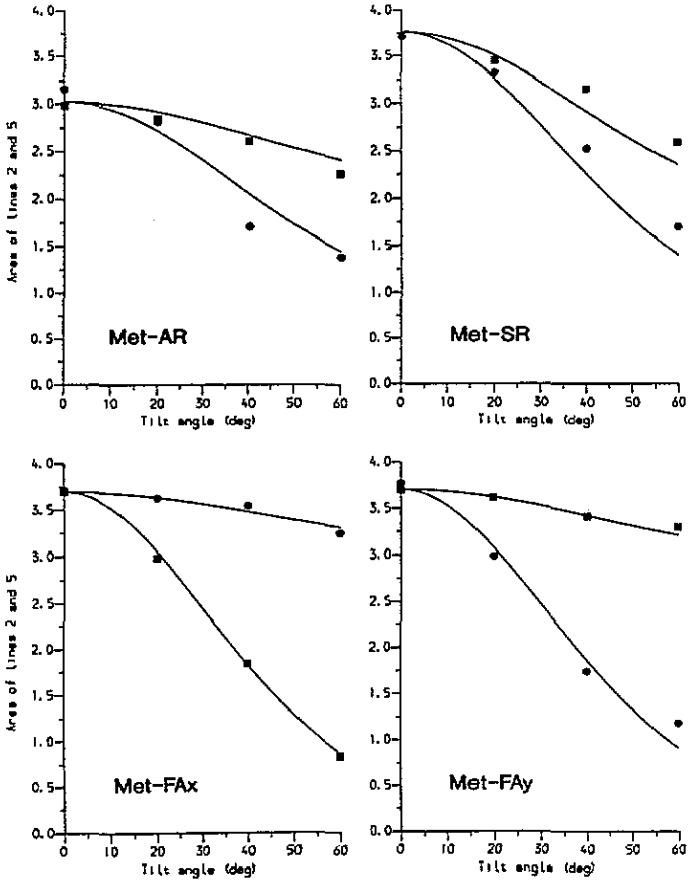

Figure 3. The relative area, r, of the second and fifth lines in the Mössbauer spectra of $Fe_{78}B_{13}Si_9$ (METGLAS 2605-S2), as a function of the angle of inclination between the incoming γ-ray beam and the normal to the ribbon plane (the z axis). Individual graphs refer to the post-production treatment of the samples: as-received (AR), stress-relieved (SR), field-annealed $\|x$ (FAx), and field-annealed $\|y$ (FAy). Filled squares correspond to inclination angles in the xz plane, and filled circles correspond to inclination angles in the yz plane. The solid lines are the results of least-squares fits using the wedge-shaped moment distribution model.

correspond to the ratio

$$3(1 + \langle\cos^2\theta_\gamma\rangle) : 4\langle\sin^2\theta_\gamma\rangle : (1 + \langle\cos^2\theta_\gamma\rangle) \tag{1}$$

where $\langle\cos^2\theta_\gamma\rangle$ is the mean value of the cosine of the angle between the γ-ray beam and the magnetic moments. If all the moments are aligned parallel to the γ-rays, $\langle\cos^2\theta_\gamma\rangle = 1$, and a 6:0:2 spectrum will result, whereas if all the moments are perpendicular to the γ-rays, $\langle\cos^2\theta_\gamma\rangle = 0$ and a 3:4:1 spectrum will result. In the metallic glass spectra, where the area ratio is fitted as $3:r:1$,

$$r = 4\langle\sin^2\theta_\gamma\rangle/(1 + \langle\cos^2\theta_\gamma\rangle) \tag{2}$$

may take values from 0 to 4. Thus the fact that $r = 4$ is not observed in any of the METGLAS and VAC ribbons implies that the moments are never co-planar, and there is always an out-of-plane contribution to the moment distribution. The fact that the maximal values of r

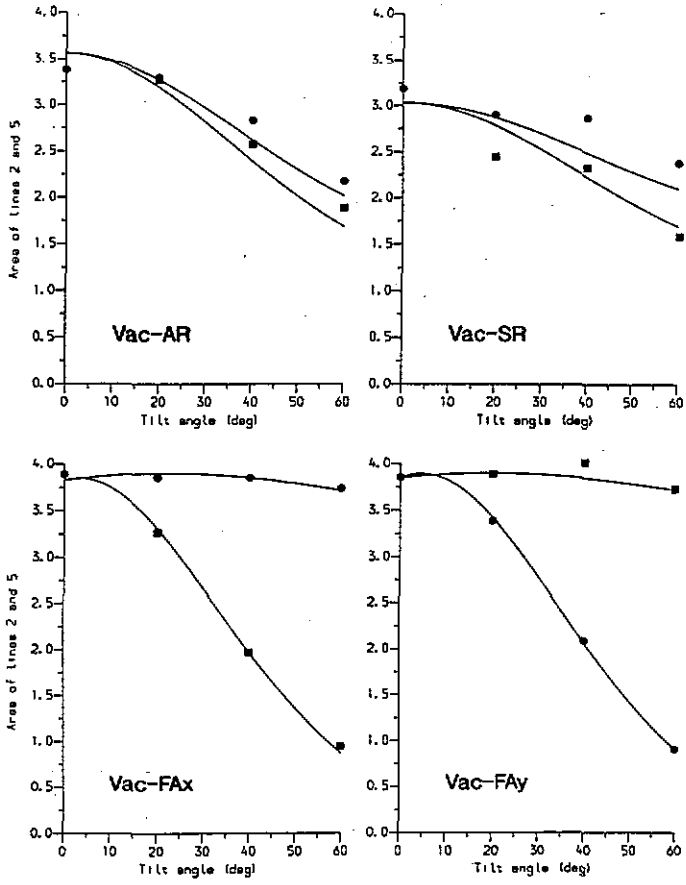

Figure 4. As in figure 3, for the $Fe_{40}Ni_{40}B_{20}$ (VAC 0040) samples. The solid lines are the results of least-squares fits using (i) the wedge-shaped moment distribution model for the as-received and stress-relieved data, and (ii) the two-moment domain model for the field-annealed data.

are observed for $\psi = 0°$ implies that in general the moments lie close to the plane of the ribbon. Thirdly, the inequivalence of the r values for inclinations of the γ-rays in the xz and yz planes shows that the moment distribution is not symmetric about the z axis.

Further analysis of the $r(\psi_{xz}, \psi_{yz})$ data was performed by least-squares fitting the data using four different moment distribution models. The parameters resulting from these fits, along with the corresponding chi-squared relative figures of merit, are summarized in table 2.

Before going into detail, it may be noted that the results summarized in table 2 demonstrate an internal consistency based on simple magnetostatic and anisotropy arguments. It is well established that the as-received material has a complex stress distribution, and given positive saturation magnetostriction, there is a complex anisotropy distribution. The angles determined from any model fit show that the moments are highly non-collinear. If the sample is stress-relieved, to a first approximation the material should become isotropic in the ribbon plane. The tabulated data show a significant reduction in the out-of-plane component of magnetization. The field anneal is designed to introduce a uniaxial anisotropy, and again the data show that the mean direction in the ribbon plane is closer to uniaxial after such a treatment. The finer detail of the results do however contain

Table 2. Parameters obtained by least-squares fitting the Mössbauer data for the METGLAS 2605-S2 and VAC 0040 ribbons using four different moment distribution models: (i) a single uniform moment (section 3.1), with polar angles θ_M and ϕ_M; (ii) an ellipsoidal distribution (section 3.2), with principal axes N_X, N_Y and N_Z; (iii) a wedge-shaped distribution (section 3.3), with an out-of-plane angular limit of u_0 and an in-plane angular limit, with respect to either the x or y axes, of v_0; and (iv) a domain model (section 3.4) with two equally probable moment directions θ_{M1}, ϕ_{M1} and θ_{M2}, ϕ_{M2}. Values of the chi-squared figure of merit, χ^2, normalized against the best fit obtained among all four models, are also quoted. All angles are measured in the xyz coordinate system, where x is the long axis of the ribbon, y is the transverse axis, and z is the normal to the ribbon plane.

(a) METGLASS 2605-S2, $Fe_{78}B_{13}Si_9$

(i) *Uniform moment model, section 3.1*

Treatment	θ_M	ϕ_M	χ^2
As received	78°	55°	7.2
Stress relieved	92°	53°	1.4
Field annealed $\|x$	87°	21°	15
Field annealed $\|y$	87°	67°	4.9

(ii) *Ellipsoidal distribution model, section 3.2*

Treatment	N_X	N_Y	N_Z	χ^2
As received	0.29	0.58	0.13	1.2
Stress relieved	0.34	0.63	0.03	1.2
Field annealed $\|x$	0.85	0.11	0.04	1.2
Field annealed $\|y$	0.13	0.83	0.04	1.1

(iii) *Wedge-shaped distribution model, section 3.3*

Treatment	u_0	v_0	Axis	χ^2
As received	40°	65°	y	1.0
Stress relieved	18°	67°	y	1.0
Field annealed $\|x$	20°	35°	x	1.0
Field annealed $\|y$	20°	39°	y	1.0

(iv) *Two-moment domain model, section 3.4*

Treatment	θ_{M1}	ϕ_{M1}	Area	θ_{M2}	ϕ_{M2}	Area	χ^2
Field annealed $\|x$	78°	16°	1.0	101°	27°	1.0	1.7
Field annealed $\|y$	78°	117°	1.0	100°	111°	1.0	1.9

(b) VAC 0040, $Fe_{40}Ni_{40}B_{20}$

(i) *Uniform moment model, section 3.1*

Treatment	θ_M	ϕ_M	χ^2
As received	90°	42°	3.4
Stress relieved	83°	36°	6.7
Field annealed $\|x$	93°	15°	1.0
Field annealed $\|y$	94°	75°	2.8

(ii) *Ellipsoidal distribution model, section 3.2*

Treatment	N_X	N_Y	N_Z	χ^2
As received	0.52	0.42	0.06	1.3
Stress relieved	0.57	0.30	0.13	1.3
Field annealed $\|x$	0.93	0.06	0.01	2.9
Field annealed $\|y$	0.08	0.91	0.01	17

(iii) *Wedge-shaped distribution model, section 3.3*

Treatment	u_0	v_0	Axis	χ^2
As received	25°	81°	x	1.0
Stress relieved	39°	67°	x	1.0
Field annealed $\|x$	7°	26°	x	2.4
Field annealed $\|y$	8°	29°	y	14

(iv) *Two-moment domain model, section 3.4*

Treatment	θ_{M1}	ϕ_{M1}	Area	θ_{M2}	ϕ_{M2}	Area	χ^2
Field annealed $\|x$	85°	11°	1.0	101°	19°	1.0	1.4
Field annealed $\|y$	88°	75°	1.0	101°	76°	1.0	1.0

important information, and full data analysis is important as we discuss below.

3.1. Uniform moment model

The simplest of all possible moment distributions is the case in which all the moments are collinear, and $\langle\cos^2\theta_\gamma\rangle = \cos^2\theta_\gamma$ where θ_γ is the angle between the γ-ray beam and the single uniform moment. By analysing the $r(\psi_{xz}, \psi_{yz})$ data the direction of the uniform moment may be determined in terms of the polar angle θ_M between the moment and the z axis, and the azimuthal angle ϕ_M between the projection of the moment onto the xy plane and the x axis.

As can be seen from the χ^2 values in table 2, this model gives poor quality fits for all the as-received and stress-relieved ribbons. This is understandable, since in those samples a complex domain structure is expected to be present, and a broad distribution of moment directions is anticipated. However, in the field-annealed ribbons, where substantial induced anisotropy is thought to be present, the uniform moment model may be expected to be more realistic. In fact, this appears to be the case for the VAC ribbons, particularly for the sample annealed along the x axis, where relatively good fits were obtained. In contrast, the field-annealed METGLAS ribbons are very poorly modelled with the single moment, implying that they possess some other distribution profile.

At this point it is relevant to note that, in a transmission Mössbauer experiment, it is impossible to distinguish between a moment pointing in the direction (θ_M, ϕ_M) and a moment pointing in the direction $(\pi - \theta_M, \phi_M + \pi)$. The uniform moment model, therefore, describes only collinear moments, and contains no information on the relative numbers of parallel or antiparallel moment populations. It is therefore consistent with both a single domain and a multi-domain model of the moment directions, provided that the moments in neighbouring domains are strictly antiparallel.

3.2. Ellipsoidal distribution

One of the most mathematically rigorous models currently used to describe moment distributions in metallic glasses is the ellipsoidal model developed by Pfannes and Fischer [15]. By assuming that the distribution function may be modelled by a series expansion in spherical harmonics, Pfannes and Fischer showed that the maximum amount of information that could be extracted from a set of Mössbauer experiments utilizing an unpolarized source was contained in the expression:

$$\langle\cos^2\theta_\gamma\rangle = c_1\sin^2\theta\cos^2\phi + c_2\sin^2\theta\sin^2\phi + c_3\cos^2\theta + c_4\sin^2\theta\cos\phi\sin\phi + c_5\sin\theta\cos\theta\cos\phi + c_6\sin\theta\cos\theta\sin\phi \quad (3)$$

where $c_1+c_2+c_3 = 1$, and (θ, ϕ) are the polar angles of the γ-ray beam in the xyz coordinate system. In other words, using an unpolarized source, only five independent parameters, and a series expansion up to second order in spherical harmonics, can be determined from the Mössbauer data.

In a later paper, Greneche and Varret [16] showed that by making an appropriate change of coordinate axes, described by three parameters in the guise of Euler rotation angles, the expression may be reduced to one containing only the two remaining independent parameters:

$$\langle\cos^2\theta_\gamma\rangle = C_1\sin^2\Theta\cos^2\Phi + C_2\sin^2\Theta\sin^2\Phi + C_3\cos^2\Theta \quad (4)$$

where $C_1+C_2+C_3 = 1$, and (Θ, Φ) are the polar angles of the γ-ray beam in the new XYZ coordinate system. In this formalism, the parameters C_1, C_2 and C_3 may be identified with the principal axes, N_X, N_Y and N_Z, of the ellipsoid that represents the moment probability distribution function.

As a first approximation, the data in figures 3 and 4 were fitted using this model under the assumption that the XYZ coordinate system could be mapped directly onto the ribbon's xyz coordinate system. This is tantamount to assuming that the moment distributions will exhibit mirror plane symmetry in the xy, xz and yz planes.

Relatively good quality fits are obtained for all the non-annealed samples, as well as for the field-annealed METGLAS ribbons. This is consistent with the expectations of broad distributions in the non-annealed ribbons, and with the earlier indications of non-collinear moments in the annealed METGLAS samples. Almost identical distributions, with interchanged values of N_X and N_Y, are obtained for the METGLAS samples field annealed parallel to x and parallel to y, implying the same degree of induced anisotropy in the two ribbons. Relatively poor fits were obtained for the annealed VAC samples, which again is consistent with the results of the uniform moment fits, where a higher degree of collinearity was suggested.

3.3. Wedge-shaped distribution

Although the ellipsoidal model is generally thought to be a realistic model for at least the as-received and stress-relieved ribbons, there are aspects to it which are counter-intuitive. In particular, as long as N_Z is non-zero, there will always be some proportion of the moments that will be predicted to be directed perpendicular to the ribbon plane. This would require a higher degree of local anisotropy than would a simple out-of-plane canting of the moments. Similarly, in field-annealed samples, a non-zero minor axis within the ribbon plane infers that some moments lie perpendicular to the induced anisotropy direction.

An alternative moment distribution model, which overcomes these concerns, is the wedge-shaped model introduced by Melamud *et al* [6]. The probability distribution is assumed to be centred on either the x or the y axis in the ribbon plane. All moment directions within a wedge-shaped region bounded by an out-of-plane angle u_0 (measured from the xy plane towards the z axis) and an in-plane angle v_0 are taken to be equally probable. The relative line areas are then found from

$$\langle \cos^2 \theta_\gamma \rangle = a \cos^2 \psi + c(1-a) \sin^2 \psi \tag{5}$$

where ψ is the polar angle of the γ-ray beam relative to the z axis, in either the xz or yz planes, and

$$a = \tfrac{1}{3} \sin^2 u_0 \qquad c = (v_0 \pm \tfrac{1}{2} \sin 2v_0)/2v_0 \tag{6}$$

where the $\pm$ sign determines which axis in the ribbon plane the moments are distributed about [5]. If $\psi = \psi_{xz}$, the plus sign is used if the moments are distributed about the x axis, and the minus sign if they are distributed about the y axis. Similarly, if $\psi = \psi_{yz}$, the plus sign signifies a distribution about the y axis, and the minus sign a distribution about the x axis.

On fitting the $r(\psi_{xz}, \psi_{yz})$ data using the wedge-shaped distribution model, χ^2 values of order 10–25% smaller than those reached using the ellipsoidal model were obtained for all the samples (see table 2). Once again relatively good fits were obtained for all except the field-annealed VAC samples. In all cases the degree of in-plane spread in moment directions

was consistent with the relative magnitudes of N_X and N_Y as found from the ellipsoid fits, as was the identification of the preferred axis in the ribbon plane. On the other hand, at first sight the degree of out-of-plane spread in moment directions seems rather large. For example, u_0 is of order 20° for the annealed METGLAS ribbons, compared with the ellipsoid fits which gave small N_Z values, of order 0.04, which imply that the moment distributions are almost planar. However, there is actually no contradiction. The relatively large out-of-plane spread in the wedge-shaped distribution is necessary to accomplish the observed reduction in r from its maximal value of 4. This same reduction is achieved within the ellipsoidal model as the result of the finite number of moments directed parallel to the γ-rays, and thereby contributing $r = 0$ to the observed relative area.

3.4. Two-moment domain model

Of the three models tested so far, the wedge-shaped distribution appears to be most appropriate for all the METGLAS ribbons, and for the non-annealed VAC ribbons. The field-annealed VAC ribbons are more accurately described by the uniform moment model. However, a more refined model may be constructed by taking into account some recent experimental work on the domain structure in field-annealed VAC 0040 ribbons [8, 17, 18]. The Bitter domain patterns clearly show domain walls parallel to the field-annealing direction, separating large domains of width $\sim$ 0.1–1 mm. In addition, a secondary wall system is evident, in which finely spaced walls lie across the larger domains, running perpendicular to the annealing direction. These secondary domains have widths $\sim$ 10–40 μm. Similar domain patterns have also been observed in METGLAS 2605-CO, $Fe_{67}Co_{18}B_{14}Si$ [9]. A schematic diagram of the postulated domain structure is given in figure 5.

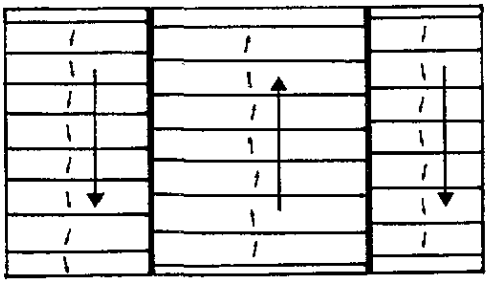

Figure 5. Schematic diagram of the domain pattern inferred from Bitter domain imaging studies of field-annealed VAC 0040 ribbons [8, 18]. The small arrows represent the moment directions in the secondary domains, and the large arrows indicate the mean moment directions in the primary domains.

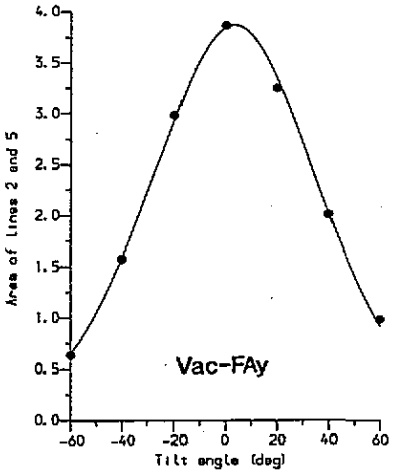

Figure 6. Relative area of the second and fifth lines in the Mössbauer spectra of the VAC 0040 ribbon that was field-annealed parallel to the y axis, as a function of the inclination angle, in the yz plane, between the γ-ray beam and the z axis. The solid line is the result of a least-squares fit using the two-moment domain model. The inequivalence of the data for positive and negative inclination angles confirms that in this sample the moment distribution does not exhibit mirror symmetry in the ribbon plane.

Although the Bitter patterns shed light on the surface domain structure only, it is reasonable to assume that the secondary domains could remain coherent throughout the 25 μm thickness of the ribbon. This assumption has been found to be accurate within 20% by Squire *et al* [18], who compared measured magnetization curves with those deduced from the observed domain structures. Consequently, a simple model of the moment distribution in the field-annealed samples may be constructed, in which there are two equally probable uniform moment directions, (θ_{M1}, ϕ_{M1}) and (θ_{M2}, ϕ_{M2}). The moment directions in neighbouring secondary domains would then alternate between (θ_{M1}, ϕ_{M1}) and (θ_{M2}, ϕ_{M2}), while the directions in neighbouring primary domains would alternate between (θ_M, ϕ_M) and $(\pi - \theta_M, \phi_M + \pi)$.

The results of fits of the field-annealed samples using this model are given in table 2. Good fits were obtained, especially for the VAC sample that was annealed along the y axis. For this sample the fitted domain moment directions seem quite reasonable, giving an out-of-plane canting of alternately $+2°$ and $-11°$, although it should be noted that this result is contrary to the supposition that the moment distribution would exhibit mirror symmetry with respect to the ribbon plane. This particular result has been checked by extending the Mössbauer experiments to include data from both positive and negative inclination angles, i.e. by recording data for $-60° \leqslant \psi \leqslant +60°$. The result of this experiment is shown in figure 6. The relative area r is indeed different for positive and negative inclination angles. For example, for $\psi_{yz} = +60°$ the relative area is $r = 0.98$, while for $\psi_{yz} = -60°$ the relative area is $r = 0.64$. The solid line in figure 6 is a refined fit to all the available data for this sample, and corresponds to $(\theta_{M1}, \phi_{M1}) = (86°, 82°)$ and $(\theta_{M2}, \phi_{M2}) = (101°, 66°)$.

The fits obtained for the field annealed METGLAS ribbons are not as good as those obtained with either the ellipsoidal or the wedge-shaped distribution models.

4. Discussion

The solid lines superimposed on the $r(\psi_{xz}, \psi_{yz})$ data in figures 3 and 4 correspond to the adjudged best fits obtained using the four alternative moment distribution models described above. It is clear from visual inspection that whereas the fits for the field-annealed samples are reasonably good, those obtained for the non-annealed samples are poor. The implication of this is that none of the proposed models is truly applicable to the non-annealed samples, in which case the nature of the moment distribution in those samples remains in some doubt. A more realistic model would probably need to be rather complicated, incorporating both distributions in the moment directions and some sort of step-function model to describe the random maze-pattern domains commonly seen in these non-annealed ribbons.

The observation that none of the proposed models could properly fit the data from the non-annealed samples is itself an important result, particularly since it is currently common practice to assume that either the ellipsoidal or the wedge-shaped distribution model is a valid representation of the moment distribution, to be trusted and tested against a limited number of data points. For example, recent determinations of the moment distributions in as-cast $Fe_{80}Cr_2Si_4B_{14}$, using the ellipsoidal model [19], and in as-received METGLAS 2605-S2, using the wedge-shaped distribution model [4], relied on the Mössbauer data from just three different inclination angles. Although this is a perfectly sensible procedure within the bounds of the respective models—it can be seen from equations (4) and (5) that three data points actually over-determine the distribution parameters—it is of concern that any discrepancy may go unnoticed unless more data points are considered.

Given the relatively good fits to the field-annealed data, it appears that the moment distribution in the VAC $Fe_{40}Ni_{40}B_{20}$ ribbons is well described by two equally populated

domains. This result is in keeping with Bitter domain imaging experiments, where a secondary domain wall system was observed in addition to the usual 180° primary domain walls. Within each secondary domain the spins are collinear, but the moment directions in neighbouring secondary domains are separated by a few degrees. The Mössbauer data provide a quantitative measurement of this angular separation, namely $\sim 18°$ for the x axis annealed ribbon, and $\sim 22°$ for the y axis annealed ribbon. In both ribbons the mean moment directions were tilted slightly out-of-plane, by $\sim 4°$. This may simply be due to a misalignment of the annealing fields.

In contrast, in the METGLAS $Fe_{78}B_{13}Si_9$ ribbons, the wedge-shaped distribution model provides the best fit to the data. On the face of it this lends support to suggestions that the moment correlation lengths in this material may be as short as the interatomic spacings. However, it is important to recall that the Mössbauer data contain no intrinsic information regarding questions of scale. For example, the wedge-shaped distribution of moments might equally well result from a two domain structure, analogous to that in the VAC ribbons, but within which the moment direction in the secondary domains wander, with respect to the mean moment direction, over different macroscopic regions of the sample. This latter hypothesis may be tested by recording Mössbauer spectra from very localized regions of the ribbon. Preliminary results from such an experiment, in which spectra were collected through a 500 μm diameter hole in a lead mask, do show discernible differences between the data collected from different parts of the ribbon [20]. Thus, it appears that the macroscopic domain structure of the ribbon being studied should be considered prior to interpreting the Mössbauer data. The question of the appropriate moment correlation lengths in these alloys remains to be resolved.

As a result of this study, we conclude that the information contained in the Mössbauer spectra of metallic glasses may be reliably analysed to obtain indications of the nature of their moment distributions, provided a sufficiently large data set is collected, so that the proper testing of hypotheses may be carried out. In further experiments we intend to implement a polarized Mössbauer source, with which it should be possible to extract more information regarding the moment directions in these materials. Keeping in mind the polarized neutron results, we also intend to study the moment distributions in metallic glass ribbons subjected to *in situ* applied magnetic fields.

Acknowledgments

We are grateful to C D Graham Jr, A P Thomas, P T Squire and R A Cowley for discussions on this subject, and to S Betteridge for recording the Mössbauer data used in figure 6. A further programme of experiments using polarized Mössbauer spectroscopy is supported by the UK Science and Engineering Research Council.

Note added in proof. (1) Subsequent to the work described in this paper, we have found evidence from x-ray diffraction measurements that all of the VAC samples had small amounts of surface crystallization present. This may be a contributing factor in the observed difference between the moment distributions in the FeNi-based VAC samples and those in the Fe-based METGLAS samples. (2) We have recently developed a further model for the moment distribution which comprises a double-Gaussian distribution [21], which may be regarded as a more physically realizable version of the wedge-shaped distribution model. The model provides fits of equal quality to that of the wedge distribution model. For the field-annealed METGLAS ribbons an in-plane Gaussian standard deviation $\sim 22°$ and an out-of-plane standard deviation $\sim 12°$ was obtained.

References

[1] Cowley R A, Patterson C, Cowlam N, Ivison P K, Martinez J and Cussen L D 1991 Non-collinear magnetic structures of Fe-based amorphous alloys *J. Phys.: Condens. Matter* **3** 9521–37

[2] Cowley R A, Cowlam N, Ivison P K and Martiniez J 1992 The structure of Fe–Ni amorphous alloys *J. Magn. Magn. Mater.* **104–107** 159–60

[3] Harker S J and Pollard R J 1989 Is iron-rich amorphous Fe–B asperomagnetic? *J. Phys.: Condens. Matter* **1** 8269–73

[4] Ivison P K, Cowlam N, Zhong Zhuping and Williams J M 1990 Surface and bulk magnetism in ferromagnetic metallic glasses *J. Non-Cryst. Solids* **117–118** 666–9

[5] Pankhurst Q A, Gibbs M R J and Thomas A P 1992 Moment distribution in $Fe_{78}B_{13}Si_9$ ribbons by Mössbauer spectroscopy *J. Magn. Magn. Mater.* **104–107** 111–2

[6] Melamud M, Swartzendruber L J, Bennett L H, Cullen J and Wun-Fogle M 1987 Moment distribution in amorphous magnetic ribbons by Mössbauer measurements *J. Appl. Phys.* **61** 3644–6

[7] Bucholtz F, Koo K P, Dandridge A and Sigel G H Jr 1986 Easy axis distribution in transversely annealed Metglas 2605-S2 *J. Magn. Magn. Mater.* **54–57** 1607–8

[8] Thomas A P and Gibbs M R J 1992 Anisotropy and magnetostriction in metallic glasses *J. Magn. Magn. Mater.* **103** 97–110

[9] Smith R H, Jones G A and Lord D G 1988 Domain structures in rapidly annealed $Fe_{67}Co_{18}B_{14}Si_1$ *IEEE Trans. Magn.* **MAG-24** 1868–70

[10] Kronmüller H and Grimm H 1977 High-field susceptibility and the spin-wave spectrum of $Fe_{40}Ni_{40}P_{14}B_6$ alloys *J. Magn. Magn. Mater.* **6** 57–60

[11] Graham C D Jr and Gibbs M R J 1993 High-field magnetization of metallic glasses *INTERMAG '93 (Stockholm, 1993) IEEE Trans. Magn.* submitted

[12] Brand R A 1987 Improving the validity of hyperfine field distributions from magnetic alloys, part II: polarized source and spin texture *Nucl. Instrum. Methods* B **28** 417–32

[13] Pollard R J 1989 Mössbauer analysis of spin directions in magnetic recording media: the problem of line area measurements *J. Appl. Phys.* **66** 3392–5

[14] Lines M E and Eibschütz M 1983 Correlation effects in the Mössbauer spectra of amorphous metallic magnetic materials *Solid State Commun.* **45** 435–9

[15] Pfannes H D and Fischer H 1977 The texture problem in Mössbauer spectroscopy *Appl. Phys.* **13** 317–25

[16] Greneche J M and Varret F 1982 On the texture problem in Mössbauer spectroscopy *J. Phys. C: Solid State Phys.* **15** 5333–44

[17] Gibbs M R J 1993 The effect of large spread in moment directions on anisotropy and magnetostriction in amorphous alloys *Proc. 5th Int. Conf. Physics of Magnetic Materials (Madralin, Poland, 1990)* at press

[18] Squire P T, Thomas A P, Gibbs M R J and Kuzminski M 1992 Domain studies of field-annealed amorphous ribbon *J. Magn. Magn. Mater.* **104–107** 109–10

[19] Miglierini M and Sitek J 1992 Mössbauer study of the spin orientation along the length of the amorphous FeCrSiB ribbon *Solid State Commun.* **82** 321–4

[20] Pankhurst Q A, McCammon C A and Gibbs M R J 1993 Moment canting in metallic glass ribbons using spatially resolved Mössbauer spectroscopy *INTERMAG '93 (Stockholm, 1993) IEEE Trans. Magn.* submitted

[21] Jiang J Z, Pankhurst Q A and Gibbs M R J 1993 A double Gaussian approach to the moment distribution in amorphous metals *ICAME '93 (Vancouver, 1993) Hyperfine Interact.* submitted